

Effects of collisions against thermal impurities in the dynamics of a trapped fermion gas

P. Capuzzi,¹ P. Vignolo,¹ F. Toschi,² S. Succi,² and M. P. Tosi¹

¹INFM-NEST and Classe di Scienze, Scuola Normale Superiore, I-56126 Pisa, Italy

²Istituto per le Applicazioni del Calcolo, CNR, Viale del Policlinico 137, I-00161 Roma, Italy

We present a theoretical study of the dynamical behavior of a gas made of ultracold fermionic atoms, which during their motions can collide with a much smaller number of thermal bosonic impurities. The atoms are confined inside harmonic traps and the interactions between the two species are treated as due to s-wave scattering with a negative scattering length modeling the ^{40}K - ^{87}Rb fermion-boson system. We set the fermions into motion by giving a small shift to their trap center and examine two alternative types of initial conditions, referring to (i) a close-to-equilibrium situation in which the two species are at the same temperature (well below the Fermi temperature and well above the Bose-Einstein condensation temperature); and (ii) a far-from-equilibrium case in which the impurities are given a Boltzmann distribution of momenta while the fermions are at very low temperatures. The dynamics of the gas is evaluated by the numerical solution of the Vlasov-Landau equations for the one-body distribution functions, supported by some analytical results on the collisional properties of a fermion gas. We find that the trapped gaseous mixture is close to the collisionless regime for values of the parameters corresponding to current experiments, but can be driven towards a collisional regime even without increasing the strength of the interactions, either by going over to heavier impurities or by matching the width of the momentum distribution of the impurities to the Fermi momentum of the fermion gas.

PACS numbers: 03.75.Ss, 02.70.Ns

I. INTRODUCTION

Trapped spin-polarized Fermi gases can be considered as non-interacting at ultralow temperatures since s-wave collisions are forbidden by the Pauli principle and higher-wave collisions are negligible [1]. The collisionality of such gases has been increased by mixing it either with a fermion gas in a different spin state [2, 3, 4, 5, 6] or with a Bose-Einstein condensed gas of bosonic atoms in numbers exceeding those of the fermions by a few orders of magnitude [7, 8, 9, 10, 11]. However, the collision rate of a fermion-fermion mixture at low temperatures is limited by the Pauli blocking of collisions as a result of the occupation of final states around the Fermi level and, in the case of a boson-fermion mixture, the collisionality can be strongly diminished by superfluidity of the condensate [12]. On the other hand, it has been shown by Ferlaino et al. [13] that the number of collisions increases if the bosons are thermal and this can be realized by diminishing the condensation temperature as for instance can be achieved by lowering the number of bosons. It was previously pointed out by Amoruso et al. [14] that the presence of a small number of bosonic impurities could drastically increase the collisionality of a Fermi gas, to the point of driving it from the collisionless to the collisional regime. However, the Fermi sphere is almost fully occupied in ultracold gases close to equilibrium as are realized in actual experiments, and the Pauli principle will in this case still limit the scattering against impurities. The dependence of collisionality on the presence of impurities thus needs detailed investigation.

In this work we study the collisional properties of an atomic Fermi gas interacting with a few atomic impuri-

ties. The presence of the impurities induces a damping of oscillatory motions of the gas and a shift of its natural oscillation frequencies. We focus on the collision and damping rates as functions of the concentration of impurities and of temperature for system parameters corresponding to ^{40}K - ^{87}Rb fermion-boson mixtures relevant to current experiments [13]. The effects of the momentum spread of the distribution of the impurities on the collision rate is also examined by both analytical and numerical means.

The paper is organized as follows. In Sec. II we introduce the physical system under study, while Sec. III discusses the collision rate and reports analytical results in two limiting cases, the details being presented in an Appendix. In Sec. IV we carry out Vlasov-Landau numerical simulations to examine the dynamics of the mixture. Finally, Sec. V offers some concluding remarks.

II. THE PHYSICAL MODEL

The system that we study is a spin-polarized Fermi gas in a trap containing bosonic impurities, which are free to move inside their own trap and interact with the fermions both through a mean-field potential and through collisions. The temperature of the system is finite and well below the Fermi temperature T_F , but well above the critical temperature for Bose-Einstein condensation of the impurities.

The fermionic component ($j = F$) and the bosonic impurities ($j = B$) in harmonic confining potentials $V_{\text{ext}}^{(j)}(\mathbf{r})$ are described by the one-body distribution functions $f^{(j)}(\mathbf{r}; \mathbf{p}; t)$. These obey the Vlasov-Landau kinetic

equations (VLE),

$$\partial_t f^{(j)} + \frac{\mathbf{p}}{m_j} \cdot \nabla_{\mathbf{p}} f^{(j)} - \nabla_{\mathbf{r}} U^{(j)}(\mathbf{r}; t) \cdot \nabla_{\mathbf{r}} f^{(j)} = C[f^{(F)}; f^{(B)}] \quad (1)$$

where the Hartree-Fock effective potential is $U^{(j)}(\mathbf{r}; t) = V_{\text{ext}}^{(j)}(\mathbf{r}) + g n^{(\bar{j})}(\mathbf{r}; t)$ with \bar{j} denoting the species different from j . Here we have set $g = 2\hbar^2 a/m_r$ with a being the

s-wave scattering length of a fermion-boson pair and m_r their reduced mass, and $n^{(\bar{j})}(\mathbf{r}; t)$ is the spatial density given by integration of $f^{(\bar{j})}(\mathbf{r}; \mathbf{p}; t)$ over momentum degrees of freedom. Since we deal with low concentrations of impurities we have neglected impurity-impurity interactions. In addition, collisions between spin-polarized fermions are negligible at low temperature and thus the collision integral C in Eq. (1) involves only collisions between fermions and impurities. This is given by

$$C = \frac{Z}{4(2\pi\hbar)^3} \int d^3p_2 \int d^3p_3 \int d^3p_4 \int d^3v \left[(1 - f^{(F)})(1 + f_2^{(B)}) f_3^{(F)} f_4^{(B)} - f^{(F)} f_2^{(B)} (1 - f_3^{(F)})(1 + f_4^{(B)}) \right]; \quad (2)$$

where $f^{(j)} = f^{(j)}(\mathbf{r}; \mathbf{p}; t)$ and $f_i^{(j)} = f^{(j)}(\mathbf{r}; \mathbf{p}_i; t)$, $d_{\mathbf{r}}$ is the element of solid angle for the outgoing relative momentum $\mathbf{p}_3 = \mathbf{p}_4$, $\mathbf{v} = \mathbf{v}_3 = \mathbf{v}_4$ is the relative velocity of the incoming particles, and $\sigma = 4a^2$ is the scattering cross-section. The collision satisfies conservation of momentum ($\mathbf{p} + \mathbf{p}_2 = \mathbf{p}_3 + \mathbf{p}_4$) and energy ($\epsilon + \epsilon_2 = \epsilon_3 + \epsilon_4$), with $\epsilon_j = p_j^2/2m_j + U^{(j)}$.

Hereafter we shall focus on a specific mixture of experimental relevance, namely, a ^{40}K - ^{87}Rb gas with strongly attractive scattering length $a = 410$ Bohr radii. At this bare scattering length the mixture is not driven to collapse for the values of the atomic densities that we consider in this work [15]. We shall focus on the case of isotropic traps with trap frequencies $\omega_F \ll \omega_B$, chosen as the geometric average of the experimental ones [13], i.e. $\omega_F = 2\pi \times 134 \text{ s}^{-1}$ and $\omega_B = 2\pi \times 912 \text{ s}^{-1}$.

III. THE COLLISION RATE

The physical observable that identifies the dynamical regime of the gas is the quantum collision rate γ_q . In

the collisionless regime the atoms collide only rarely and we have $\gamma_q \ll \omega_j$, while if $\gamma_q \gg \omega_j$ the gas is in a collisional regime which can be well described by hydrodynamic equations. In the general case a kinetic treatment is necessary such as the one used in this work. The collision rate can then be evaluated either from a numerical simulation which actually counts the number of collisions at each time step, or by direct integration of the collision integral C over momenta. Numerical simulation runs for the problem at hand will be presented in Sec. IV.

In the second type of approach that we have mentioned above, the starting point is the usual assumption that before a collision the distribution functions for the incoming particles and for the occupancy of the final states are the equilibrium Fermi and Bose distributions. The local collision rate γ_q^{loc} is then given by

$$\gamma_q^{\text{loc}} = \frac{a^2 m_r^3}{(2\pi\hbar)^6} \int d^3p_i \int d^3v_i \int d\cos\theta_i \int d\cos\theta_f f_1^{(F)} f_2^{(B)} (1 - f_3^{(F)})(1 + f_4^{(B)}); \quad (3)$$

Here \mathbf{p}_i and \mathbf{v}_i are the total momentum and the relative velocity of the incoming particles, and θ_i (θ_f) is the direction of the relative velocity of the incoming (outgoing) particles in the scattering plane. At equilibrium the Fermi and Bose distributions in Eq. (3) are given by

$$f_i^{(j)} = \exp[-(\epsilon_i^{(j)} - \mu^{(j)})/k_B T] \quad (4)$$

where $j = 1$ or 2 respectively for fermions and bosons, $\mu^{(j)}$ are the chemical potentials, and $T = 1/k_B T$. The

total number of instantaneous collisions occurring in the system per unit time is then calculated as $\gamma_q = \gamma_q^{\text{loc}} \int d^3r$.

One can further develop the evaluation of Eq. (3) in two limiting cases (see Appendix). In the first case the temperature T of the fermions is very low – more precisely, $T \ll T_F$ where $T_F = (6N_F)^{1/3} \hbar^2/m_F$ is the Fermi temperature and $T_c = 0.94 N_B^{1/3} \hbar^2/m_B = k_B T_c$ is the critical temperature for Bose-Einstein condensation, with

N_F and N_B being the numbers of particles of the two species. In Eq. (3) we can then replace $f^{(F)}$ by the zero-temperature Fermi distribution and $f^{(B)}$ by a classical distribution of the form

$$f^{(B)}(r;p) = \frac{1}{3=2} \frac{1}{p_0^3} n_B(r) e^{-p^2/p_0^2} \quad (5)$$

where $n_B(r)$ is the local density and p_0 the momentum spread of the impurities.

The parameter p_0 is crucial in determining the scattering rate in this situation. When the momentum spread of the impurities is low, i.e. for $p_0 = p_F \rightarrow 1$ where $p_F = \sqrt{2m_F \epsilon_F}$, all collisions are forbidden by the Pauli principle since any fermionic final state which would be allowed by kinematics belongs to the Fermi sphere. Collisions involving empty fermionic final states become possible on increasing p_0 and the collision rate starts increasing. At the same time the volume occupied by the impurities in the trapped system also increases and γ_q reaches a maximum value when the two clouds have approximately the same size, i.e. for $p_0 = m_B \sqrt{2} p_F = (m_F \sqrt{2})$. On an additional increase of p_0 the effective number of impurities that can interact with the fermions goes down and consequently the number of collisions decreases. In this latter limit $p_0 = p_F \rightarrow 1$, the leading term of the local collision rate is calculated in the Appendix and leads to the result

$$\gamma_q \sim \frac{8}{a^2} \frac{m_B^2 \sqrt{2}}{p_0^3} N_B N_F \quad (6)$$

A more direct estimate in the same limit is obtained by a classical evaluation of the collision rate through the relation $\gamma_q = v N_F N_B$ with the impurity density $N_B = N_B (m_B \sqrt{2} p_0)^3 = (4/3)$. The relative velocity v_i can be set to $p_0 = m_B$ and we get

$$\gamma_q \sim 3a^2 \frac{m_B^2 \sqrt{2}}{p_0^3} N_B N_F \quad (7)$$

which is in good agreement with Eq. (6). Equations (6) and (7) show that the collision rate rises for heavier impurities, thus favoring a collisionless-to-collisional dynamical transition. One may consider using in this context not only atomic impurities but also e.g. heavier stable molecules.

The second limiting case in which progress can be made by analytical means refers to a gas at high temperature, it is worth noticing that in this case there would be no difference in considering as impurities either bosons or fermions. The behavior of the mixture approaches that of a classical two-component uid, where the number of collisions per unit time is

$$c_l = \frac{k_r^{3=2}}{2} \frac{1}{m_r^{1=2}} N_B N_F \quad (8)$$

(see Appendix). In Eq. (8) $k_r = m_B \sqrt{2} m_F \sqrt{2} = (m_B \sqrt{2} + m_F \sqrt{2})$ is the reduced oscillator strength.

Finally, in close-to-equilibrium situations the evolution of the fermions can be obtained from a first-order approximation on the collision integral as

$$C = -\frac{d}{dt} f_0^{(F)} \quad (9)$$

where $f_0^{(F)}$ is the equilibrium distribution. The quantity determines the damping rate of oscillatory motions of the fermions and at low collisionality an order-of-magnitude estimate of the damping can be obtained by evaluating one of the terms entering the full collision integral (see e.g. [16]). This yields a relationship between collision rate and damping rate as

$$\gamma_q = N_F \quad (10)$$

The accuracy of this relation will be explored numerically in the next Section.

IV. DYNAMICS OF THE FERMIONS

The analysis of the dynamics of the mixture requires the solution of the VLE in Eq. (1). The solution is obtained by using a fully three-dimensional concurrent code with numerical procedures which are essentially the same as those described in Refs. [17, 18] for a two-component Fermi gas, except for the choice of the initial phase-space distributions and for the bosonic enhancement factors entering the collision integral. The details have already been given elsewhere [18].

We shall analyze two different experiments. In the first, the mixture is prepared in an equilibrium state with distribution functions as given in Eq. (4). In the second experiment the fermionic and bosonic clouds are prepared independently at two different temperatures (T and T_B) and are then superposed in space. In this case the fermions obey a phase-space distribution given by Eq. (4) with a vanishing mean-field term, while the impurities are distributed according to Eq. (5) with $p_0 = (2m_B T_B)^{1=2}$.

A. Dynamics near to equilibrium

Having prepared the mixture in an equilibrium state inside isotropic traps, the system is set off by giving a slight displacement to the center of the fermion trap. We count the collisions made per unit time and per fermion, and report its average during roughly 8 oscillations. Therefore, at variance from what was discussed in Section III, the collision rate calculated in this way includes both the effects of the instantaneous collisions and of the dynamics.

In Fig. 1 we report the scaled collision rate γ_q and (in the inset) the collision rate γ_q as functions of $N_B = N_F$ at $N_F = 10^5$, for three values of the temperature below the Fermi temperature. We are dealing in these cases

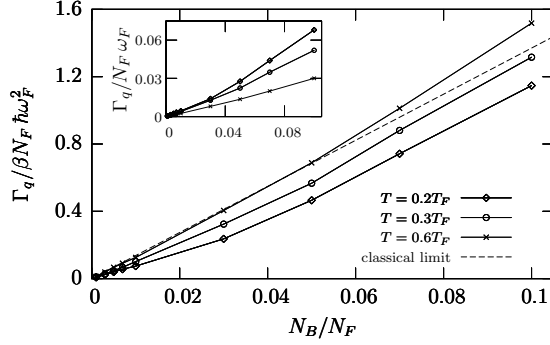


FIG. 1: Scaled collision rate $\Gamma_q = N_F$ per fermion (in units of $\hbar \omega_F^2$) in a $^{40}\text{K}-^{87}\text{Rb}$ mixture in isotropic confinement with $N_F = 10^5$, as a function of the impurity concentration $N_B = N_F$ at three values of the temperature $T = T_F$ (symbols). The dashed line shows the classical limit of Eq. (8). The inset shows the collision rate $\Gamma_q = N_F$ per fermion, in units of $\hbar \omega_F^2$.

with almost classical impurities ($T = T_c \approx 1.2 - 1.6$) giving a very small contribution to the mean-field potential. The collisionality of the gas obviously decreases with N_B and goes linearly to zero for vanishing N_B . The effect of cooling the gas is instead more subtle. In spite of Pauli blocking the collision rate increases on cooling (see inset), as a result of the increase of the density of impurities in the overlap region of the two clouds. This effect has the same origin as the factor entering the classical collision rate in Eq. (8) and indeed the scaled quantity Γ_q decreases on cooling, as is shown in the main body of Fig. 1. This also shows that the classical formula in Eq. (8) gives a good account of our results at $T = 0.6 T_F$ (see also Ref. [19]). Similar trends are obtained in simulation runs at $N_F = 10^4$.

We have also analyzed the damping rate of the oscillations of the fermion cloud under the influence of the impurities and its relationship with the collision rate. With the present system parameters the gas is close to the collisionless regime, as is demonstrated by displaying in Fig. 2 the relationship between γ and Γ_q for isotropic confinement. The damping rate was obtained from the simulation data by fitting the center-of-mass coordinate of the fermions to the expression $z_F(t) / \cos(\omega_F t) \exp(-\gamma t)$. It is seen from Fig. 2 that the first-order estimate given in Eq. (10) for a fluid at low collisionality is not far from our numerical results. For what concerns the dependence of γ on temperature, we see from Fig. 2 that it is closely related to that of Γ_q since in this type of plot the data for different temperatures are essentially superposed.

B. Dynamics far from equilibrium

We focus on an experiment in which, instead of varying the number of impurities or the shape of the trap, we can control the distribution of the impurities. In practice this

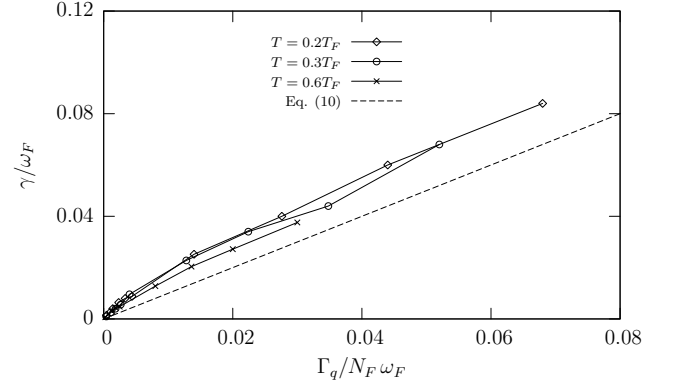


FIG. 2: Damping rate γ (in units of ω_F) in a $^{40}\text{K}-^{87}\text{Rb}$ mixture in isotropic confinement with $N_F = 10^5$, as a function of the collisionality $\Gamma_q = N_F \hbar \omega_F^2$ per fermion (cf. Fig. 1) and at three values of T (symbols). The dashed line shows the first-order approximation given in Eq. (10).

could be realized by preparing spatially separated clouds and then rapidly transferring them into the same spatial region. This situation is closer to the system discussed in Ref. [14], where strongly out-of-equilibrium collisions were assumed. Being an out-of-equilibrium situation we choose to characterize the dynamics by displaying the time-averaged collision rate of the system as function of p_0 .

The collision rate per fermion as a function of the momentum spread of the impurities is shown in Fig. 3. Here the time-averaged results from simulation runs on a Fermi gas at $T = 0.3 T_F$ are compared with those from the numerical integration of Eq. (3) for a fully degenerate Fermi gas ($T = 0$) at equilibrium and from its analytical expansion at large p_0 as given in Eq. (6). Even though there are quantitative differences between the results at $T = 0$ and $T = 0.3 T_F$, the qualitative behavior is the same at both temperatures and the discrepancies could be attributed to the enhancement of the collisionality at higher T and to out-of-equilibrium effects missing in Eq. (3). The peak near $p_0 \approx p_F$ corresponds to the situation where the two clouds essentially occupy the same spatial region. Correspondingly, in view of Eq. (10) also the damping rate will have a peak at the same point. On further increasing the momentum spread p_0 the effective number of impurities that interact with the fermions diminishes and consequently the collision and damping rates decrease.

Figure 4 shows the time-averaged ratio $\hbar \Gamma_q / \gamma$ between the quantum and the classical collision rates as a function of $T_B = T_F$, as estimated during the simulation in correspondence to the data points in Fig. 3. Almost all collisions allowed by kinematics for $p_0 > p_F$ involve empty fermionic final states so that Pauli blocking is ineffective. For $p_0 < p_F$ instead, only impurities in the tail of the momentum distribution can contribute to the collision rate and the Pauli suppression increases dramatically. The quantum suppression is still lower than in

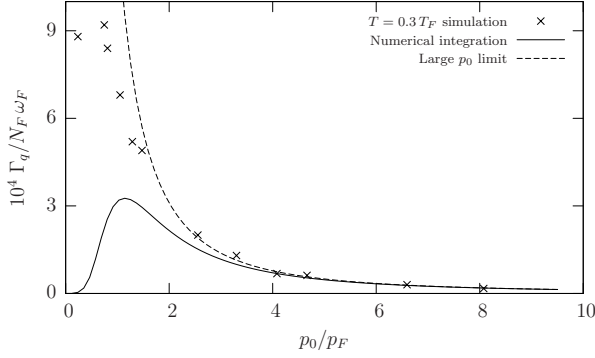


FIG. 3: Collision rate per fermion (in units of $10^4 \Gamma_q / N_F \omega_F$) as a function of the momentum spread p_0 (in units of the Fermi momentum p_F) for $N_F = 10^4$ ^{40}K atoms and $N_B = 100$ ^{87}Rb impurities inside spherical traps.

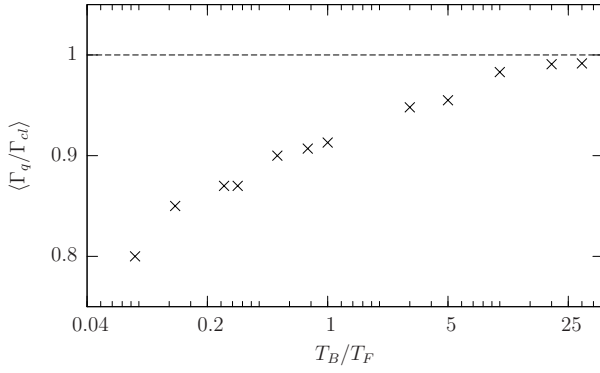


FIG. 4: Time-averaged ratio $h_q = c_l$ between the quantum and the classical collision rate at $T = 0.3 T_F$, obtained in the numerical simulation as a function of T_B/T_F (in log scale) for the gas shown in Fig. 3.

the case of a two-component mixture of fermions, where both components are subject to Pauli blocking. In this case $h_q = c_l$ has been estimated to be roughly 0.65 at $T = 0.3 T_F$ [19], while in the present case of bosonic impurities we find $h_q = c_l \approx 0.9$ for $T_B = 0.3 T_F$ (see Fig. 4).

V. SUMMARY AND CONCLUDING REMARKS

We have studied the collisionless properties of a spin-polarized Fermi gas interacting with a small number of thermal bosonic impurities and have focused on two related aspects of its collisionality, i.e. the collision rate and the damping rate of oscillations. While the superfluidity of Bose-condensed atoms lowers the collisionality of Bose-Fermi mixtures and the Pauli principle operating in a second fermionic component blocks collisional events in Fermi-Fermi mixtures, the use of thermal bosons circum-

vents these limitations and may offer a feasible method to increase the collisionality of a spin-polarized fermion gas.

For near-to-equilibrium dynamics in ^{40}K - ^{87}Rb mixtures similar to those used in actual experiments at LENS [13] we have found that collisions are rare and that the gas is close to the collisionless regime. We have suggested that some parameters characterizing the system could be tuned to increase its collisionality and thus drive the system towards the collisional regime. We have also shown how in a far-from-equilibrium experiment on a fermion gas at $T \approx 0$ the addition of bosonic impurities with momentum spread around the Fermi momentum p_F could induce an enhancement of collisionality. Due to the dependence of the collision rate on the mass of the impurities, a further increase of collisionality could be achieved by choosing as impurities heavy particles such as ^{133}Cs [20] and ^{172}Yb [21] atoms, or strongly bound molecules.

Finally, the trap anisotropy could be raised so that for cigar-shaped traps the axial oscillations would be damped more rapidly than the radial ones on their own time scale. The system could thus be driven into the intermediate collision regime on increasing the anisotropy of the trap. The transition from the collisionless to the collisional regime as driven by anisotropy will be investigated in detail in future work [22].

Acknowledgments

This work has been partially supported by an Advanced Research Initiative of Scuola Normale Superiore di Pisa and by the Istituto Nazionale di Fisica della Materia within the Advanced Research Project "Photon matter" and the initiative "Calcolo Parallelo".

APPENDIX A: SOME ANALYTICAL RESULTS

1. High temperature

At high temperature the local collision rate in a two-component mixture with only inter-species interactions is given by the classical expression

$$\Gamma_{cl}^{loc}(\mathbf{r}) = \int d^3p_1 d^3p_2 v f^{(1)}(\mathbf{r}; p_1) f^{(2)}(\mathbf{r}; p_2) \quad (\text{A1})$$

where v is the relative velocity of particles 1 and 2 and the classical distribution functions in an anisotropic trap are

$$f^{(j)}(\mathbf{r}; \mathbf{p}) = \frac{N_j}{(2\pi)^3} e^{-\frac{\mathbf{p}^2}{2m_j} + U^{(j)}(\mathbf{r})} \quad (\text{A2})$$

Integration of Eq. (A1) is straightforward and gives

$$\frac{\text{loc}}{\text{cl}}(x) = \frac{1}{2^{\frac{5=2}{7=2}}} \frac{(m_1 m_2)^{3=2}}{m_r^{1=2}} N_1 N_2 (!_1 !_2)^3 e^{V_{\text{ext}}^{(1)}(x) + V_{\text{ext}}^{(2)}(x)} \quad (\text{A } 3)$$

if mean-field potentials can be neglected. The total collision rate can then be calculated by evaluating the integral of Eq. (A 3) over space. This yields Eq. (8) for the classical collision rate.

of the momentum spread p_0 . In this case the fermionic distribution is the Fermi-Dirac step function, while the impurities are taken thermally distributed according to Eq. (5). Neglecting the Bose enhancement factor and mean-field effects, ρ_q^{loc} can be written as

2. Low temperature and large momentum spread of bosonic impurities

The collision rate can also be analytically estimated when the fermions are at $T \rightarrow 0$ and for large values

$$\begin{aligned} \log_q(r) = & a^2 \frac{m_1 m_2}{2m_r} \frac{B(r)}{3=2h^3 p_0} \mathbb{R} \, dP_i e^{\frac{m_1^2 p_i^2}{2} \frac{p_i^2}{p_0^2}} \mathbb{R} \, dv_i v_i e^{\frac{m_1^2 v_i^2}{2} \frac{p_i^2}{p_0^2}} e^{\frac{m_1^2}{2} \frac{p_i^2}{p_0^2}} e^{\frac{m_1^2}{2} \frac{p_i^2}{p_0^2}} e^{\frac{p_i^2 + m_1^2 v_i^2}{2} \frac{p_i^2}{p_0^2}} e^{2 \frac{m_1^2}{2} \frac{p_i v_i}{p_0^2}} \end{aligned} \quad (\text{A } 4)$$

where the integration bounds in v_i , i.e. $v = p_{i \rightarrow m_2}$ and $v_+ = (p_{i \rightarrow m_2} + p_{r \rightarrow m_r})$, come from requiring that the final states in a collision are unoccupied.

To obtain the number of collisions per unit time we integrate the above expression inside the Thomas-Fermi radius R_{TF} of the fermion cloud. This is defined as the classical turning point of a fermion with energy ϵ_{F} in the external trapping potential, i.e.

$$R_{TF} = \frac{S \frac{2}{m_F} \langle F \rangle}{m_F + F} \quad (A5)$$

where we set $\langle F \rangle$ at the non-interacting value $\langle F \rangle = p_F^2/2m_F = (6N_F)^{1/3} \hbar^2/F$. On increasing p_0 the inte-

grand in Eq. (A 4) is well approximated by an inverted parabola with zeroes at v_- and v_+ , and hence the integral over v_1 is trivial. We obtain

$$\frac{1}{q} \log_q(r), \quad \frac{4}{3} \frac{a^2}{m_2} \frac{B(r)}{3=2h^3} p_0 p_F^3 : \quad (A 6)$$

Expression (6) in the main text follows from taking a local-density approximation for p_F by setting $p_F =$

$2m_F \langle V_{\text{ext}}^{(F)}(r) \rangle$ and performing the space integration of the local collision rate in Eq. (A 6).

- [1] A. M. Inguzzi, S. Succi, F. Toschi, M. P. Tosi, and P. Vignolo, *Phys. Rep.* 395, 223 (2004).
- [2] B. Demarco and D. S. Jin, *Science* 285, 1703 (1999).
- [3] S. D. Gensemer and D. S. Jin, *Phys. Rev. Lett.* 87, 173201 (2001).
- [4] S. R. Ganade, M. E. Gehm, K. M. O'Hara, and J. E. Thomas, *Phys. Rev. Lett.* 88, 120405 (2002).
- [5] S. Jochim, M. Bartenstein, G. Hendl, J. Hecker-Denschlag, R. Grimm, A. Mosk, and M. Weidemüller, *Phys. Rev. Lett.* 89, 273202 (2002).
- [6] K. Dieckmann, C. A. Stan, S. Gupta, Z. Hadzibabic, C. H. Schunck, and W. Ketterle, *Phys. Rev. Lett.* 89, 203201 (2002).
- [7] A. G. Truscott, K. E. Strecker, W. I. M. Alexander, G. B. Partridge, and R. G. Hulet, *Science* 291, 2570 (2001).
- [8] F. Schreck, L. Khaykovich, K. L. Corwin, G. Ferrari, T. Bourdel, J. Cubizolles, and C. Salomon, *Phys. Rev. Lett.* 87, 080403 (2001).
- [9] G. Roati, F. Riboli, G. Modugno, and M. Inguscio, *Phys. Rev. Lett.* 89, 150403 (2002).
- [10] J. G. Okwiri, S. B. Papp, B. Demarco, and D. S. Jin, *Phys. Rev. A* 65, 021402 (2002).
- [11] Z. Hadzibabic, C. A. Stan, K. Dieckmann, S. Gupta, M. W. Zwierlein, A. G. Orlicz, and W. Ketterle, *Phys. Rev.*

- Lett. 88, 160401 (2002).
- [12] E. Timmermans and R. Côte, Phys. Rev. Lett. 80, 3419 (1998).
 - [13] F. Ferlaino, R. J. Brecha, P. Hannaford, F. Riboli, G. Roati, G. Modugno, and M. Inguscio, J. Opt. B 5, S3 (2003).
 - [14] M. Amoruso, I. Maccioli, A. Minguzzi, and M. P. Tosi, Eur. Phys. J. D 7, 441 (1999).
 - [15] G. Modugno, G. Roati, F. Riboli, F. Ferlaino, R. J. Brecha, and M. Inguscio, Science 297, 2240 (2002).
 - [16] K. Huang, Statistical Mechanics (Wiley, New York, 1987).
 - [17] F. Toschi, P. Vignolo, S. Succi, and M. P. Tosi, Phys. Rev. A 67, 041605 (2003).
 - [18] F. Toschi, P. Capuzzi, S. Succi, P. Vignolo, and M. P. Tosi, J. Phys. B 37, S91 (2004).
 - [19] S. Succi, F. Toschi, P. Capuzzi, P. Vignolo, and M. P. Tosi, Phil. Trans. R. Soc. (2004), in press.
 - [20] T. Weber, J. Herbig, M. Mark, H.-C. Nagerl, and R. Grimm, Science 299, 232 (2003).
 - [21] Y. Takasu, K. Maki, K. Komori, T. Takano, K. Honda, M. Kumakura, T. Yabuzaki, and Y. Takahashi, Phys. Rev. Lett. 91, 040404 (2003).
 - [22] P. Capuzzi, P. Vignolo and M. P. Tosi, submitted to Laser Physics.